



Article

Physiological and Transcriptomic Analyses Reveal the Response of Medicinal Plant *Bletilla striata* (Thunb. ex A. Murray) Rchb. f. via Regulating Genes Involved in the ABA Signaling Pathway, Photosynthesis, and ROS Scavenging under Drought Stress

Hai Liu ¹, Kaizhang Chen ², Lin Yang ¹, Xue Han ¹, Mingkai Wu ^{1,*} and Zhijun Shen ^{3,*}

¹ Institute of Modern Chinese Herbal Medicines, Guizhou Academy of Agricultural Sciences, Guiyang 550025, China

² Science and Technology Bureau of Pengyang County, Guyuan 756500, China

³ Fujian Key Laboratory of Subtropical Plant Physiology and Biochemistry, Fujian Institute of Subtropical Botany, Xiamen 361006, China

* Correspondence: bywmk1999@163.com (M.W.); shenzj1987@xmu.edu.cn (Z.S.)



Citation: Liu, H.; Chen, K.; Yang, L.; Han, X.; Wu, M.; Shen, Z.

Physiological and Transcriptomic Analyses Reveal the Response of Medicinal Plant *Bletilla striata* (Thunb. ex A. Murray) Rchb. f. via Regulating Genes Involved in the ABA Signaling Pathway, Photosynthesis, and ROS Scavenging under Drought Stress. *Horticulturae* **2023**, *9*, 307. <https://doi.org/10.3390/horticulturae9030307>

Academic Editors: Giuliana Maddalena, Annamaria Mincuzzi, Francesca Garganese and Antonio Ippolito

Received: 24 November 2022

Revised: 10 February 2023

Accepted: 20 February 2023

Published: 23 February 2023



Copyright: © 2023 by the authors. Licensee MDPI, Basel, Switzerland. This article is an open access article distributed under the terms and conditions of the Creative Commons Attribution (CC BY) license (<https://creativecommons.org/licenses/by/4.0/>).

Abstract: *Bletilla striata* is a valuable Chinese herbal medicinal plant widely used in various fields. To meet the market demand for this herb, the tissue culture technology of *B. striata* was developed. However, drought stress has been a significant threat to the survival of cultivated *B. striata*. To further understand the underlying mechanisms of *B. striata* under drought stress, its response was investigated at the physiological and transcriptional levels. Our photosynthesis results show that the decline of the net photosynthesis rate (P_n) in *B. striata* leaves was mainly caused by nonstomatal limitation factors. Using transcriptomic analysis 2398, differentially expressed genes (DEGs) were identified. KEGG enrichment analysis showed that DEGs involved in plant hormone signal transduction (ko04075) were significantly altered, especially the abscisic-acid signaling pathway. The up-regulations of the serine/threonine protein kinase (*SnRK2*) and S-type anion (*SLAH2*) channels might lead to stomatal closure, which is the reason for decline of photosynthesis. Moreover, the downregulation of cytochrome b6 and photosystem I reaction center subunit III/IV might be the major reason for nonstomatal limitation. In addition, *B. striata* enhanced the ability of ROS scavenging via activating the gene expression of superoxide dismutase, catalase, and peroxidase in response to drought stress. Our study enhanced the understanding of *B. striata* in response to drought stress.

Keywords: *Bletilla striata*; medicinal plant; drought; transcriptome; ABA

1. Introduction

Drought is a critical environmental factor that seriously threatens plant growth and development [1]. Drought stress hampers various biological processes in plants, such as photosynthesis, cell elongation, nutrient uptake, and reproduction [2–6]. Plants have evolved a battery of defense mechanisms to ensure their survival and fitness in the face of a drought.

One plant response to drought is to reduce stomatal apertures so that leaf water potential is maintained [7]. While it restricts water from exiting, stomatal closure also restricts CO₂ from entering, thereby reducing the photosynthesis rate. Reactive oxygen species (ROSs) are also produced from photosynthesis and photorespiration [8]. The restriction of the photosynthesis rate caused by stomatal closure leads to overproduction of toxic ROS, which disrupts the electron transport system and starves cellular organelles of their carbon feedstock [7]. These toxic compounds cause oxidative damage that limits plant growth and development [8]. In response to this, a cell would synthesize antioxidants such

as catalase (CAT), superoxide dismutase (SOD), peroxidase (POX), ascorbate peroxidase (APX), glutathione (GSH), and glutathione sulfo-transferase (GST) [9]. The biosyntheses of these complex antioxidants form the primary defense line against drought stress [10–12].

As a valuable Chinese herbal medicine, *Bletilla striata* (Thunb. ex A. Murray) Rchb. f. has received increasing attention from scholars in the last decade. The *Bletilla striata* polysaccharide (BSP) is the important component in the *B. striata* tuber, purported to accelerate localized hemostasis in the lungs and stomach [13,14]. The development of omics technology enabled us to further explore the potential application value of *B. striata*. With bioinformatic analyses of the transcriptome data, auxin/indole-3-acetic acid (*Aux/IAA*) genes were suggested to participate in *B. striata* tuber development [15]. Similarly, another transcriptomic study proposed a pathway for BSP biosynthesis [16]. Recently, the genome of *B. striata* was sequenced and analyzed, and it will enhance molecular marker-assisted breeding of *B. striata* to improve traits of medicinal value [17]. These studies provide a solid foundation for *B. striata* planting and engineering of breeding for the future.

Although *B. striata* is widely distributed in China, the current industry of foraging *B. striata* from the wilderness is unable to meet the market demand not only due to its long growth periods and low breeding efficiency but also because it is widely used in various fields [18,19]. To solve this problem, the tissue culture technique was applied to successfully breed tissue culture seedlings [20]. However, the seedlings suffered from dehydration when they were transplanted to greenhouses and fields. Recently, a study found that PYLs-PP2C22/38-SnRK2s function as the ABA core signal pathway in response to multiple abiotic stresses [21]. Another study of *B. striata* suggested that an appropriate drought condition could improve its growth [22]. However, the mechanism of *B. striata* in response to drought stress is not well-known. To better understand the underlying mechanism of the *B. striata* response to drought stress, physiological and transcriptomic analyses were performed in the present study.

2. Materials and Methods

2.1. Plant Growth and Drought Treatment

Bletilla striata seedlings were produced through tissue culturing at the Institute of Modern Chinese Herbal Medicines, Guizhou Academy of Agricultural Sciences (Guizhou, China). Three seedlings with similar sizes (22–26 cm height, with 3 leaves) were transplanted into one pot (15 cm height × 14 cm diameter). A mixture of humus, vermiculite, and sand (1:1:1, *v:v:v*) was used as a soil matrix. Every twelve pots were put in a box (each group contained 36 seedlings at least). The seedlings were grown in a greenhouse at a daily temperature of 26–28 °C, a light intensity of 500–800 $\mu\text{mol}\cdot\text{m}^{-2}\cdot\text{s}^{-1}$, a photoperiod of 12/12 h (day/night), and a relative humidity of 50–80%. After two weeks of cultivation in the greenhouse, healthy seedlings were randomly divided into two groups (CK and drought).

At the beginning of the drought treatment, the plot containing soil matrix was fully irrigated with tap water and put in a greenhouse until no water came out from the bottom of the plot. Then, the weight of the soil was recorded (g_1). The soil was dried out until its weight was stable (g_2). Subsequently, soil water content was calculated with the following formula: soil water content = $(g_1 - g_2)/g_2 \times 100\%$. Afterward, a certain amount of water (g_3) was added to the soil (soil water content = $g_3/(g_2 + g_3) \times 100\%$). Then, the *B. striata* seedlings were transplanted into these plots. The seedlings were irrigated with tap water every three days to maintain the soil water content at 25–35% (CK) or 5–10% (drought) for four weeks. Soil water content was real-time-monitored using time-domain reflectometry (Field Scout TDR 100, Spectrum Technologies Inc., Aurora, CO, USA). Each group had three replicates.

2.2. Leaf Photosynthesis Measurement

The second fully expanded leaf from the top was selected for photosynthesis measurement using the portable Li-6400XT photosynthesis measurement system (Li-6400, Li-Cor,

Lincoln, NE, USA). This test measured the net photosynthetic rate (P_n), intercellular CO_2 concentration (C_i), stomatal conductance (G_s), and transpiration rate (E) of the plant. From there, the stomatal limitation (L_s) and nonstomatal limitation (C_i/G_s) were calculated using formulae described in previous studies [23,24]. For each treatment, the photosynthesis measurement was performed on at least five seedlings. The photosynthetically active radiation (PAR) was set at $500 \mu\text{mol}\cdot\text{m}^{-2}\cdot\text{s}^{-1}$, while the concentration of atmospheric CO_2 was maintained at around $400 \mu\text{mol}\cdot\text{mol}^{-1}$.

2.3. RNA Extraction, Library Construction, and Sequencing

A 0.2 g sample of a fresh leaf was ground into powder in liquid nitrogen, and the total RNA was extracted using the Trizol (Invitrogen, Carlsbad, CA, USA) method, following the instructions provided by the vendor. The RNA quality was analyzed using the RNA Nano 6000 Assay Kit of the Bioanalyzer 2100 system (Agilent Technologies, Santa Clara, CA, USA). The value of the RIN (RNA integrity number) should have been higher than 8.5, and 28S:18S should have been higher than 1.5. After RNA extraction, a cDNA library was constructed according to vendor recommendation (Illumina, San Diego, CA, USA). The total RNA was used to isolate poly-(A) mRNA with Oligo-(dT) magnetic beads. The poly-(A) mRNA was fragmented in a fragmentation buffer. M-MuLV reverse transcriptase (RNase H-) was used for first-strand cDNA synthesis. The synthesis of second-strand cDNA was catalyzed with DNA polymerase in a buffer containing dNTPs and RNaseH. The passivation of the remaining overhangs was conducted through exonuclease/polymerase activities. With adenylation of 3' ends of DNA fragments, a NEBNext adaptor with a hairpin loop structure was ligated to prepare for hybridization. The cDNA fragments with 250–300 bp lengths were purified with an AMPure XP system (Beckman Coulter, Beverly, CA, USA). Then, $3 \mu\text{L}$ of the USER enzyme (NEB, Ipswich, MA, USA) was used with size-selected, adaptor-ligated cDNA at 37°C for 15 min. This selected cDNA was amplified by the polymerase chain reaction (PCR) in the mixed solution containing Universal PCR primers, Q5 Hot Start HiFi DNA polymerase, and Index (X) primer.

The amplified DNA were purified (AMPure XP system), and the quality of the cDNA library was assessed using the Agilent Bioanalyzer 2100 system. The index-coded samples were clustered using a cBot Cluster Generation System and a TruSeq PE Cluster Kit v4-cBot-HS (Illumina, San Diego, CA, USA) according to the vendor instructions. Afterward, the library preparations were sequenced on an Illumina HiSeq 2500 platform, and 100/50 bp single-end reads were generated.

2.4. De Novo Assembly and Sequence Annotation

Raw data were initially processed through in-house perl scripts, resulting in clean data, which was defined as having a Q20 value higher than 90% per our quality assessment criteria. The clean data were assembled using Trinity software [25]. Unigenes were generated and aligned to various databases. The thresholds for the Nr, Nt, and Swiss-Prot databases were each less than 1×10^{-5} , and the thresholds for the Pfam, KOG, GO, and KEGG databases were less than 1×10^{-2} , 1×10^{-3} , 1×10^{-6} , and 1×10^{-10} , respectively.

2.5. Analyses of Differentially Expressed Genes (DEGs)

The clean data were searched against the assembled unigenes, and the read count for each unigene was calculated using the RSEM method [26]. EdgeR software was used to adjust the read counts through one scaling normalized factor. Differential expression analysis was then performed using the DEGSeq R package. The p values were adjusted using the method described by Yoav et al. [27]. The threshold of significant differential expression was q -value < 0.005 , $|\log_2(\text{fold change})| > 1$.

2.6. KEGG Enrichment Analysis of Differentially Expressed Genes

KEGG and GO (Biological process) enrichment were performed to further understand the function of differentially expressed genes (DEGs). Hypergeometric distribution was used to test the statistical enrichment of DEGs in KEGG pathways.

2.7. Statistical Analysis

The data displayed in the figures were presented as means \pm SE. The statistical significance of all data was analyzed using a univariate analysis of variance ($p < 0.05$) (one-way ANOVA; SPSS version 19.0).

3. Results

3.1. The Photosynthesis of *B. striata* under Drought Stress

After four weeks of exposure to the simulated drought condition, most of the *B. striata* leaves turned yellow and dry, and the roots were short and slim (Figure 1). As illustrated in Figure 2, for the drought-treated plants, a gradual decrease in net photosynthetic rate (P_n), stomatal conductance (G_s), and transpiration rate (E) was recorded throughout the four weeks, except for a sharp decline from days 14 to 21. In addition, the intercellular CO_2 concentration (C_i) gradually increased in the drought treatment but did not significantly change in the CK. Further analysis showed that the value of stomatal limitation, L_s , gradually decreased, while the nonstomatal limitation, C_i/G_s , sharply increased from days 14 to 21, which suggested that the plant had incurred serious cellular damage after 21 days of drought condition.

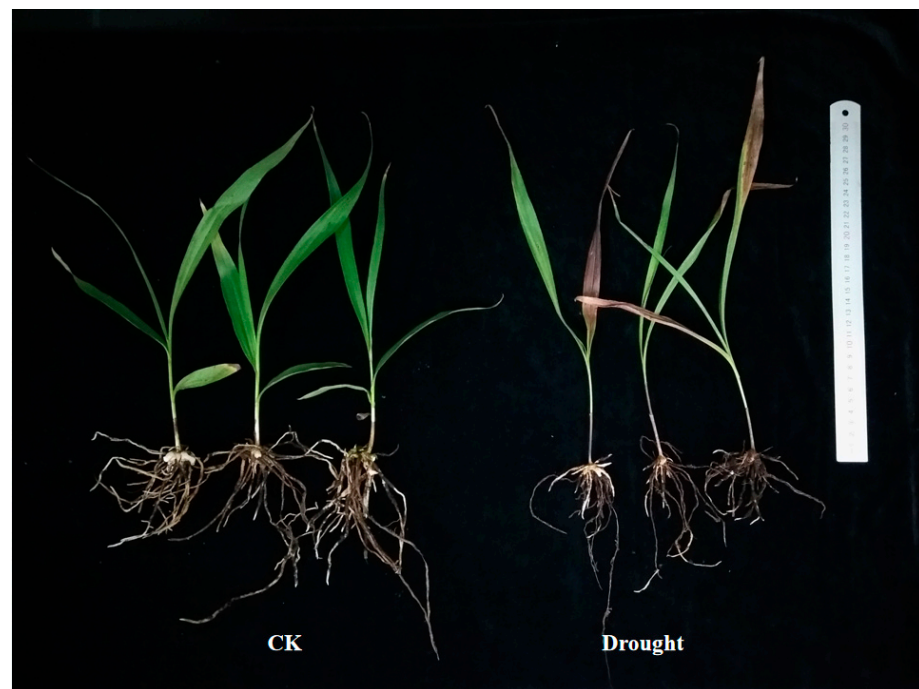


Figure 1. Images of *B. striata* under normal (CK) and drought conditions.

3.2. De Novo Assembly, Quality Assessment, and Annotation of Transcriptome

To further investigate the mechanisms that regulate the drought response of *B. striata*, Illumina RNA-Seq sequencing was performed in the present study. Totals of 51,068,510, 47,394,690, 49,121,326, 45,204,114, 56,709,020, and 55,046,454 paired-end reads (150 bp) were obtained in CK1, CK2, CK3, drought1, drought2, and drought3, respectively (Table 1). After removal of the adapter and the low-quality reads, 49,902,994, 46,355,072, 48,119,710, 44,225,174, 55,207,808, and 53,905,350 clean reads were retained in CK1, CK2, CK3, drought1, drought2, and drought3, respectively (Table 1). The value of Q30 in each sample was more

than 90%, implying that the clean data were of high quality and could be used for further analysis (Table 1). To assess the reproducibility of the CK and the drought treatments, the Pearson analysis was performed in this study. The results showed that values of R^2 among CK1, CK2, and CK3 ranged from 0.75 to 0.79, while the values among drought1, drought2, and drought3 ranged from 0.74 to 0.80 (Figure 3). These results suggest good reproducibility in the group. Trinity software was used to assemble the clean reads de novo, and 122,160 unigenes with a 1451 bp mean length were obtained. The median length and N50 were 1044 and 2240 bp, respectively. Afterward, the unigenes were aligned to various databases. From a total of 122,160 unigenes, 81,958 (67.09%) unigenes were aligned to the Nr database, 45,174 (36.97%) unigenes were aligned to the NT database, 29,847 (24.43%) unigenes were aligned to the KO database, 57,293 (46.89%) unigenes were aligned to the SwissProt database, 56,063 (45.89%) unigenes were aligned to the PFAM database, 56,063 (45.89%) unigenes were aligned to the PFAM database, and 21,869 (17.90%) unigenes were aligned to the KOG database. In total, 86,618 (70.90%) out of the 122,160 unigenes could be aligned to at least one database (Table 2).

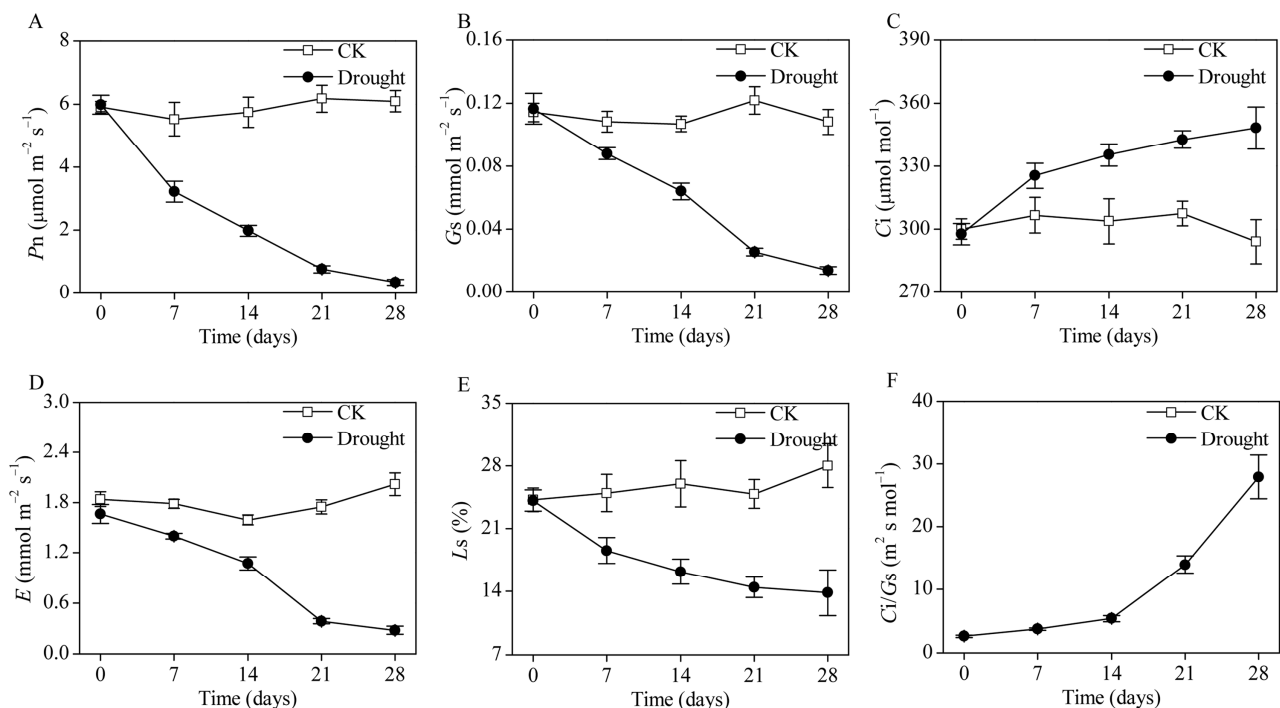


Figure 2. The photosynthetic characteristics of *B. striata* under normal and drought conditions: (A) net photosynthetic rate (P_n), (B) stomatal conductance (G_s), (C) intercellular CO_2 concentration (C_i), (D) evaporation rate (E), (E) stomatal limitation (L_s), and (F) ratio of C_i/G_s . Means and standard errors of at least five replicates are shown.

Table 1. Summary of transcriptomes in *B. striata* under drought stress.

Sample	CK1	CK2	CK3	Drought1	Drought2	Drought3
Raw Data	51,068,510	47,394,690	49,121,326	45,204,114	56,709,020	55,046,454
Clean Data	49,902,994	46,355,072	48,119,710	44,225,174	55,207,808	53,905,350
Q30 (%)	92.56	90.14	92.24	92.34	92.40	92.03
GC Content (%)	47.71	47.61	47.65	46.99	47.30	46.97

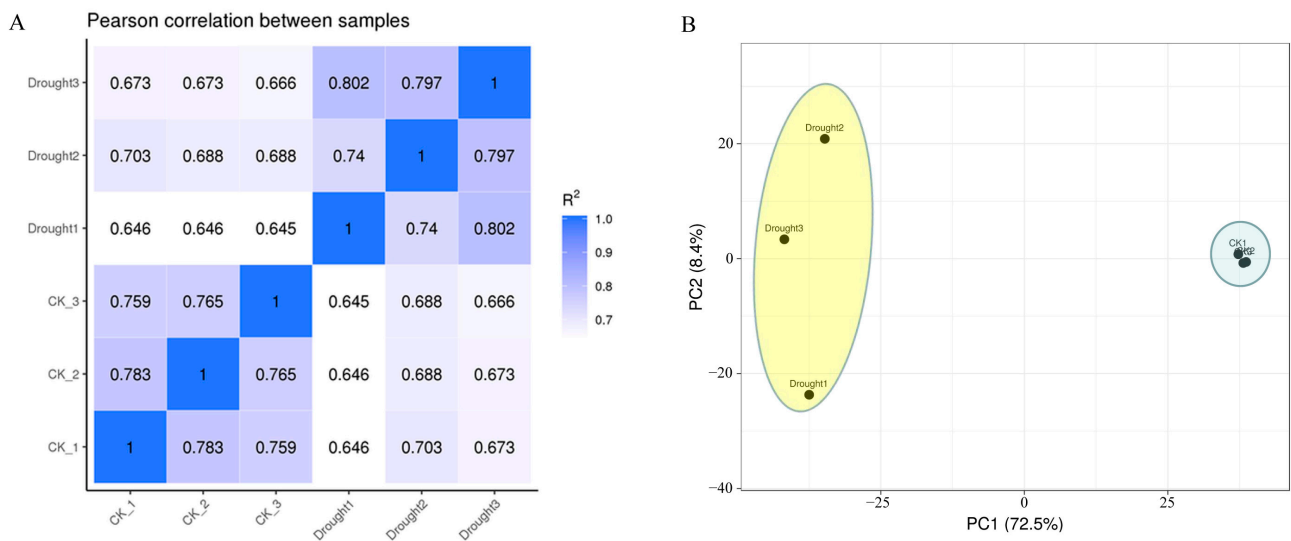


Figure 3. The Pearson correlation coefficient (A) and principal component analysis (B) of *B. striata* under CK and drought stress.

Table 2. Annotations of unigenes in various databases.

Database	Number of Genes	Percentage (%)
Annotated in NR	81,958	67.09
Annotated in NT	45,174	36.97
Annotated in KO	29,847	24.43
Annotated in SwissProt	57,293	46.89
Annotated in PFAM	56,063	45.89
Annotated in GO	56,063	45.89
Annotated in KOG	21,869	17.9
Annotated in At Least One Database	86,618	70.9

3.3. KEGG and GO Enrichment Analysis of Differentially Expressed Genes (DEGs)

To identify the differentially expressed genes (DEGs) in *B. striata* leaves under drought stress, the expression level of each DEG was calculated. A total of 2398 DEGs were identified, 1271 DEGs were upregulated, and 1127 DEGs were downregulated (Figure 4).

To further explore the underlying mechanism of the *B. striata* response to drought stress, KEGG and GO (Biological process) enrichment analyses were performed. Figure 5A shows that nine KEGG pathways ($p < 0.05$) were significantly enriched in *B. striata* exposed to drought conditions: plant hormone signal transduction (ko04075); phenylpropanoid biosynthesis (ko00940); tropane, piperidine, and pyridine alkaloid biosynthesis (ko00960); phenylalanine metabolism (ko00360); tyrosine metabolism (ko00350); starch and sucrose metabolism (ko00500); cyanoamino acid metabolism (ko00460); diterpenoid biosynthesis (ko00904); and alpha-linolenic acid metabolism (ko00592). Figure 6 presents the expression profiles of the DEGs involved in plant hormone signal transduction. Almost half of the DEGs identified in these pathways were upregulated, and the other half were downregulated, which highlighted the complicated roles of plant hormones in orchestrating the response to drought stress. Most DEGs involved in abscisic-acid signal transduction were also upregulated, such as protein phosphatase 2C (*PP2C*), abscisic acid-insensitive 5-like protein 5 (*ABF*), and serine/threonine protein kinase SAPKs (*SnRK2*).

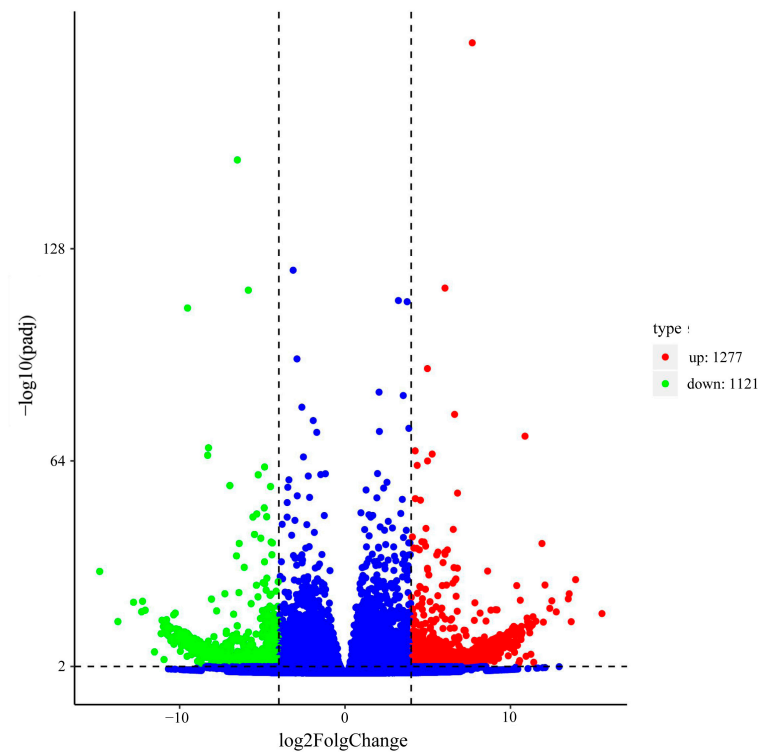


Figure 4. The volcano plot of differentially expressed genes (DEGs) in *B. striata* leaves under CK and drought conditions. Red plots represent upregulated DEGs, green plots represent downregulated DEGs, and blue plots represent the DEGs without significantly change.

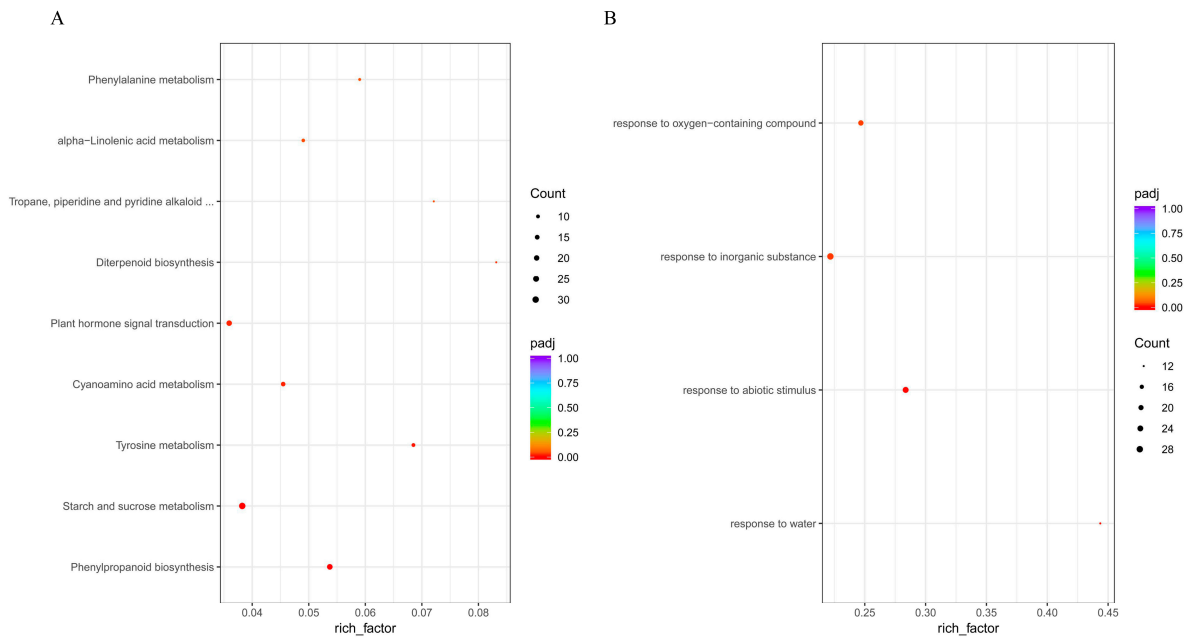


Figure 5. The KEGG and GO enrichment analyses of *B. striata* under CK and drought conditions. (A) The results of KEGG enrichment analysis; (B) the results of GO (biological process) enrichment analysis.

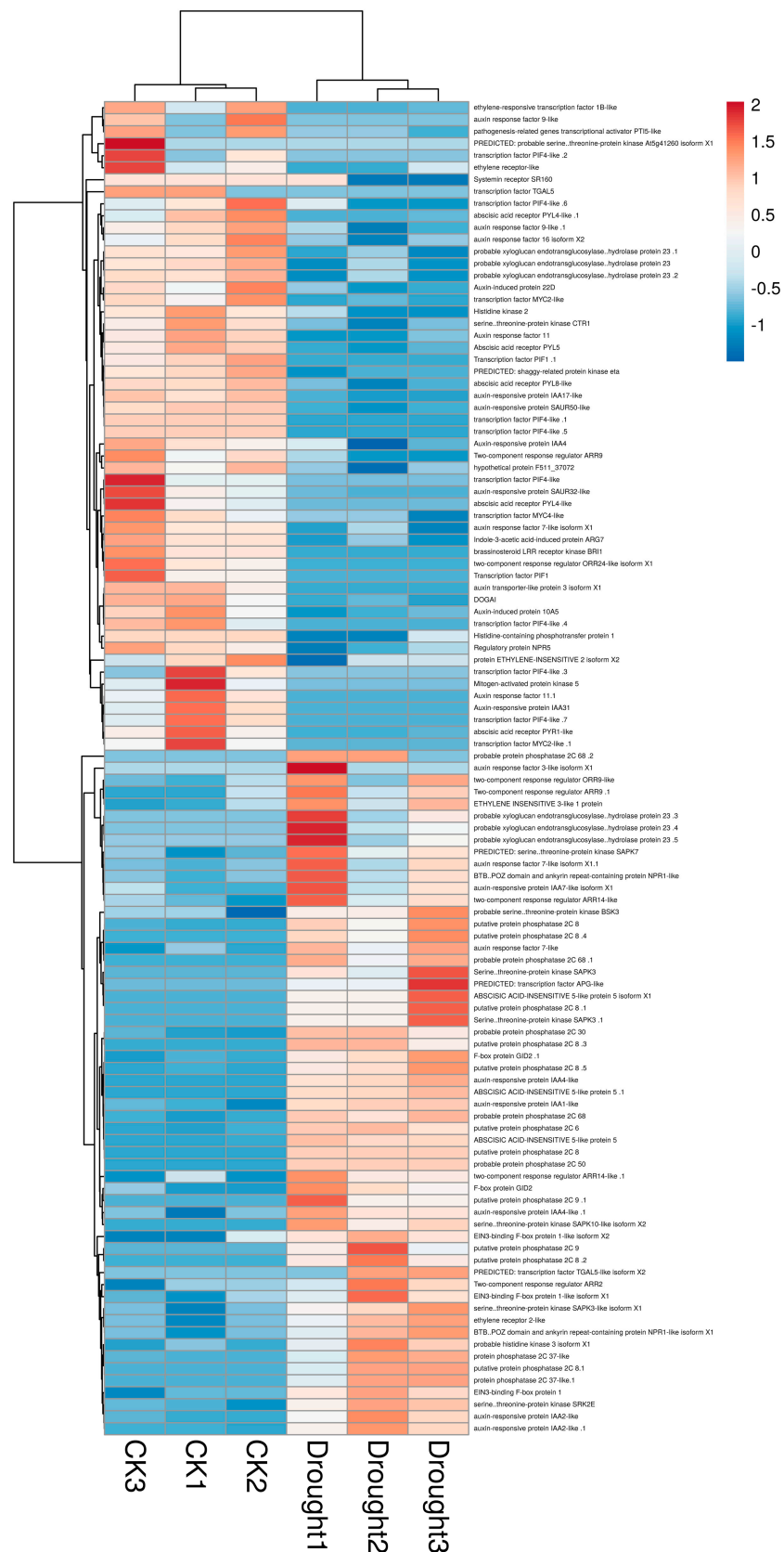


Figure 6. Hierarchical clustering analysis of DEGs involved in plant hormone signal transduction (ko04075) in *B. striata* under CK and drought conditions. Each group has three replicates.

Four GO terms ($p < 0.05$) related to stress are laid out in Figure 5B: response to water (GO:0009415), response to an abiotic stimulus (GO:0009628), response to an inorganic substance (GO:0010035), and response to an oxygen-containing compound (GO:1901700). From there, the expression patterns of DEGs related to these GO terms are presented in Figure 7. Interestingly, we found several DEGs, which encoded dehydrin proteins, were profoundly induced under drought stress (Figure 7).

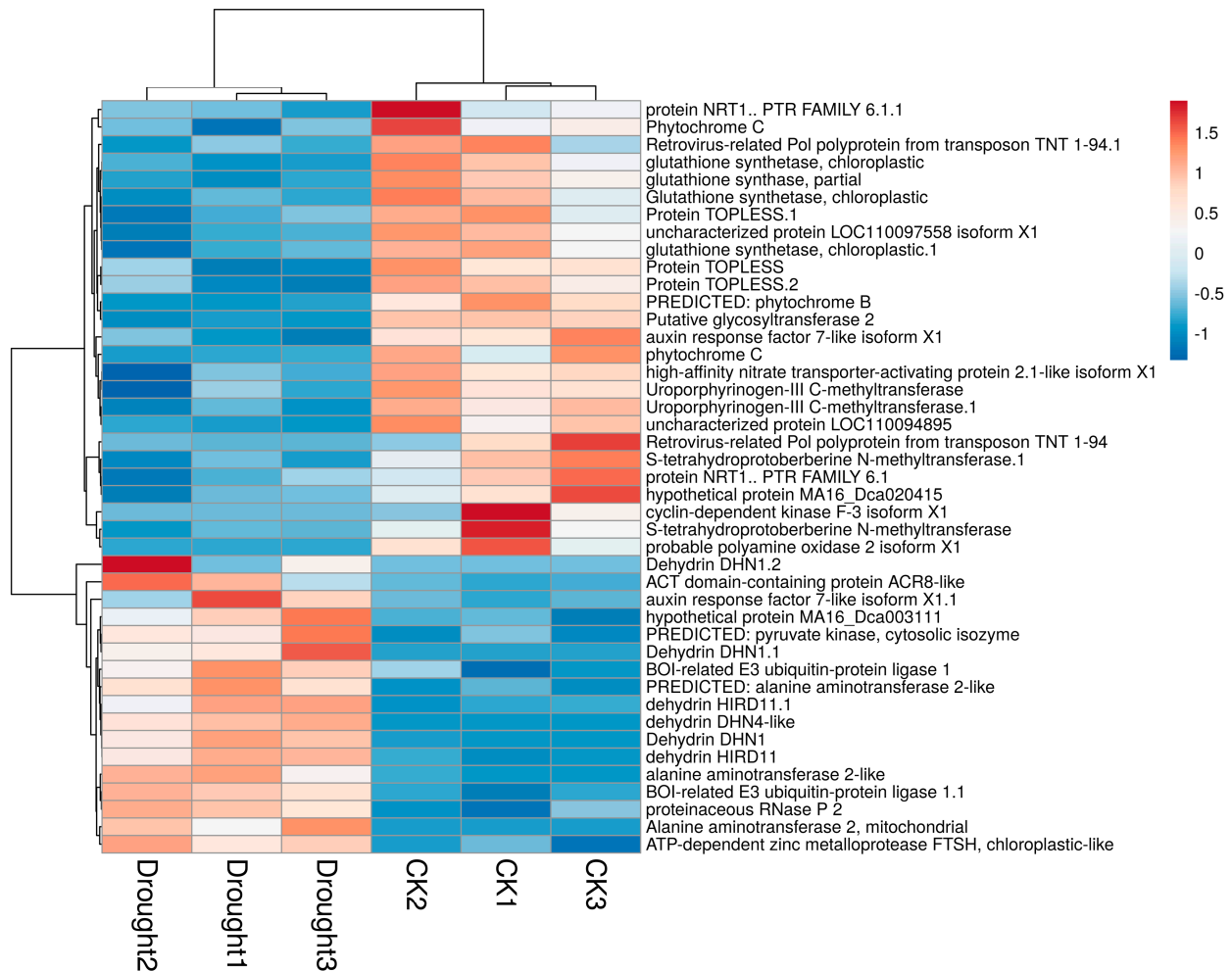


Figure 7. The expression profiles of DEGs involved in four GO terms in *B. striata* under CK and drought conditions, including response to water (GO:0009415), response to an abiotic stimulus (GO:0009628), response to an inorganic substance (GO:0010035), and response to an oxygen-containing compound (GO:1901700). Each group has three replicates.

In addition, detailed information of the DEGs, related to photosynthesis, ABA signal transduction and antioxidant metabolism, are presented in Table 3. Fourteen DEGs were involved in photosynthesis. Four DEGs (Cluster-6724.91253, Cluster-6724.49822, Cluster-6724.49802, and Cluster-6724.50075) were downregulated, and the other ten DEGs were upregulated. Five out of thirty-four DEGs (*PYLs* and *PYR*, which are ABA acceptors) were downregulated in ABA signal transduction, and twenty-nine DEGs (*PP2C*, *ABF*, and *SLAH2*) were upregulated. All DEGs in antioxidant metabolism (*SOD*, *CAT*, *POD*, and *GST*) were upregulated except for Cluster-6724.52388 and Cluster-6724.52387 (*APX*).

Table 3. DEGs related to photosynthesis, ABA signal transduction, and antioxidant metabolism in *B. striata* under drought stress.

Gene ID	NR ID	NR Description	log2FC	<i>q</i> -Value
Photosynthesis				
Cluster-6724.91253	YP_009347733.1	Cytochrome b6, chloroplast	−2.2224	0.009795
Cluster-6724.49822	XP_020586841.1	Photosystem I reaction center subunit III, chloroplastic	−1.2025	0.015406
Cluster-6724.49802	XP_020584337.1	Photosystem I reaction center subunit V, chloroplastic	−1.2516	0.000058
Cluster-6724.50075	XP_020592430.1	Photosystem I reaction center subunit psaK, chloroplastic	−1.2483	0.00262
Cluster-6724.44868	XP_020674733.1	psbQ-like protein 3, chloroplastic	7.5757	0.000007
Cluster-6724.68113	PKU73612.1	PsbP domain-containing protein 3, chloroplastic	7.6345	0.026749
Cluster-6724.86842	XP_020701207.1	psbP domain-containing protein 1, chloroplastic isoform X1	1.1728	0.000497
Cluster-6724.55459	PKU68001.1	ATP-dependent zinc metalloprotease FTSH 11, chloroplastic	6.1654	0.012827
Cluster-6724.47025	XP_020682163.1	ATP-dependent zinc metalloprotease FTSH 11, chloroplastic	7.0383	0.018672
Cluster-6724.49015	AVI16663.1	Photosystem I reaction center subunit psaK	3.4885	0.020947
Cluster-6724.74411	XP_020682631.1	Oxygen-evolving enhancer protein 2, chloroplastic-like	1.7217	0.005108
Cluster-2398.0	XP_018676095.1	PREDICTED: photosynthetic NDH subunit of luminal location 3, chloroplastic-like	5.4806	0.041334
Cluster-6724.11910	XP_020600282.1	Oxygen-evolving enhancer protein 3-2, chloroplastic-like	1.1112	0.030315
Cluster-6724.49786	XP_020672629.1	Photosystem II core complex proteins psbY, chloroplastic isoform X2	1.3762	0.000000
ABA Signal Transduction				
Cluster-6724.40260	XP_020672595.1	Abscisic-acid receptor PYL4-like	−6.9396	0.000001
Cluster-6724.91783	XP_020673631.1	Abscisic-acid receptor PYR1-like	−3.4996	0.000000
Cluster-6724.61155	XP_020587854.1	Abscisic-acid receptor PYL8-like	−1.4327	0.000000
Cluster-6724.38513	PKU64533.1	Abscisic-acid receptor PYL5	−2.9087	0.000000
Cluster-6724.40259	XP_020672595.1	Abscisic-acid receptor PYL4-like	−4.046	0.000000
Cluster-6724.61497	KZV54161.1	Hypothetical protein F511_37072	−1.5431	0.046313
Cluster-6724.3652	PKU68005.1	Putative protein phosphatase 2C 8	2.1736	0.032413
Cluster-6724.16415	PKU68005.1	Putative protein phosphatase 2C 8	3.9737	0.000260
Cluster-6724.91192	XP_020597478.1	Protein phosphatase 2C 37-like	4.6738	0.000000
Cluster-6724.6728	XP_020698862.1	Probable protein phosphatase 2C 68	4.1538	0.000000
Cluster-6724.46469	PKA58960.1	Putative protein phosphatase 2C 8	3.0705	0.000000
Cluster-6724.86228	PKA58960.1	Putative protein phosphatase 2C 8	4.132	0.01917
Cluster-6724.93558	PKU74952.1	Putative protein phosphatase 2C 9	5.5698	0.000110
Cluster-6724.93557	PKU74952.1	Putative protein phosphatase 2C 9	5.4473	0.000036
Cluster-6724.15036	XP_020682015.1	Probable protein phosphatase 2C 30	2.1485	0.000000
Cluster-6724.22798	XP_020698862.1	Probable protein phosphatase 2C 68	8.7029	0.000000
Cluster-6724.22799	XP_020698862.1	Probable protein phosphatase 2C 68	7.5918	0.000025
Cluster-6724.5916	PKU68005.1	Putative protein phosphatase 2C 8	2.9511	0.000000
Cluster-6724.5917	PKU68005.1	Putative protein phosphatase 2C 8	3.25	0.000000
Cluster-6724.5919	PKU68005.1	Putative protein phosphatase 2C 8	3.9231	0.000000
Cluster-6724.90331	XP_020597478.1	Protein phosphatase 2C 37-like	6.6068	0.000000
Cluster-6724.48042	PKU76292.1	Putative protein phosphatase 2C 6	1.9241	0.000000
Cluster-6724.69799	XP_020693557.1	Probable protein phosphatase 2C 50	5.1397	0.000052
Cluster-6724.5918	PKU68005.1	Putative protein phosphatase 2C 8	3.8178	0.000000

Table 3. Cont.

Gene ID	NR ID	NR Description	log2FC	<i>q</i> -Value
Cluster-6724.65584	XP_020573821.1	Serine/threonine protein kinase SAPK3-like isoform X1	1.0795	0.041358
Cluster-6724.50267	XP_020705528.1	Serine/threonine protein kinase SAPK10-like isoform X2	2.5198	0.000000
Cluster-6724.56769	XP_015636932.1	PREDICTED: serine/threonine protein kinase SAPK7	1.9686	0.000100
Cluster-6724.18821	PKU80471.1	Serine/threonine protein kinase SAPK3	5.6694	0.004812
Cluster-6724.60505	API65110.1	Serine/threonine protein kinase SRK2E	1.0474	0.000001
Cluster-6724.52592	PKU80471.1	Serine/threonine protein kinase SAPK3	6.8354	0.000240
Cluster-6724.41934	PKU79905.1	ABSCISIC ACID-INSENSITIVE 5-like protein 5	1.2712	0.000000
Cluster-6724.51613	XP_020694098.1	ABSCISIC ACID-INSENSITIVE 5-like protein 5 isoform X1	3.9425	0.008781
Cluster-6724.93796	PKU83951.1	ABSCISIC ACID-INSENSITIVE 5-like protein 5	3.2259	0.000000
Cluster-7290.0	PKU75117.1	S-type anion channel SLAH2	4.146	0.000001
Antioxidant Metabolism				
Cluster-6724.52388	ACN25039.1	Ascorbate peroxidase	−4.3302	0.000005
Cluster-6724.52387	ACN25039.1	Ascorbate peroxidase	−9.2054	0.000000
Cluster-6724.51106	XP_020590426.1	Superoxide dismutase [Cu-Zn] 4A	7.6369	0.000002
Cluster-6724.49968	XP_020702876.1	Catalase isozyme A	7.8841	0.000000
Cluster-4051.0	XP_020585759.1	Peroxidase P7-like isoform X1	4.5187	0.000000
Cluster-6724.2897	PKU65314.1	Peroxidase 42	4.6461	0.000000
Cluster-6724.98401	PKU59654.1	Cationic peroxidase 1	7.797	0.000086
Cluster-6724.78777	XP_020679253.1	Probable glutathione S-transferase parA	9.8673	0.000006
Cluster-6724.95492	PKU87189.1	Putative glutathione S-transferase parA	6.9382	0.003953
Cluster-6724.45643	PKU87189.1	Putative glutathione S-transferase parA	4.1034	0.002935
Cluster-15974.0	XP_020573757.1	Glutathione S-transferase F8, chloroplastic-like	4.5425	0.000004

4. Discussion

4.1. ABA Signal Transduction in *B. striata* Leaves under Drought Stress

Phytohormones regulate various biological processes to control plant growth and stress responses [28]. To survive under drought stress, plants have evolved extensive phytohormone signaling pathways in response to drought stress, such as those of auxin (IAA), cytokinin (CK), abscisic acid (ABA), jasmonic acid (JA), salicylic acid (SA), ethylene (ET), and gibberellin (GA) [29,30]. The present study identified a series of DEGs that participate in plant hormone signal transduction (ko04075) (Figures 5A and 6; detailed information for ko04075 is shown in Supplementary Table S2). Among these phytohormones, ABA was regarded as the major stress-responsive hormone under drought stress [30]. Under normal conditions, PP2C would inhibit the activity of SnRK2 protein via dephosphorylating [30]. When a plant is exposed to drought conditions, its cellular ABA concentration increases, which binds PYL/PYR/RCARs proteins. This ABA-PYL/PYR/RCARs complex would then inhibit the activity of PP2C, which would lead to the activation of SnRK2 [31,32]. The activated SnRK2 would phosphorylate downstream genes and trigger the ABA-induced response [30]. A recent study reported that PYL-PP2C-SnRK2s, which function as the ABA core signal pathway, also exist in *B. striata* [21]. Our results also showed that many DEGs engaged in ABA signal transduction (*PP2C*, *ABF*, *SnRK2*), and most of them were upregulated except for *PYL/PYR/RCARs* (Figure 6). The *SnRK2* gene is suspected to be positively related to stomatal closure, since a *srk2e* mutation in *Arabidopsis* resulted in a wilted mutant caused by a loss of stomatal closure under drought stress [33]. Upregulated *SnRK2* could activate several cation or anion channels, such as S-type anion channels (SLAHs), to force the stomata to close [34]. Based on these results, the upregulations of *SnRK2* and *SLAH2* (Table 3) in *B. striata* under drought stress suggest that drought stress might result

in promoting stomatal closure to prevent water loss from leaves via controlling ion efflux in guard cells. Mori et al. (2006) also found that ABA was initially synthesized in the roots and subsequently migrated to the leaves, where it would shut the stomata and reduce plant photosynthesis [35]. Consistently with previous studies, our results found that most of the DEGs (*PP2C*, *SnRK2*, and *SLAH2*) that participated in core ABA signaling pathway PYL-PP2C-SnRK2 were upregulated (Table 3), and the values of the net photosynthetic rate (P_n) and stomatal conductance (G_s) were decreased under drought stress (Figure 2). The same results were also reported by Liu et al. [21]; stomatal closure was gradually decreased in *B. striata* leaves with lower soil water content. The decline of P_n could have been caused by stomatal limitation (L_s) and nonstomatal limitation (C_i/G_s) [36]. Our results found a decrease in L_s but an increase in C_i/G_s in *B. striata* leaves under drought stress (Figure 2). According to the results presented above, we concluded that the decline of photosynthesis in *B. striata* leaves under drought stress is mainly caused by nonstomatal limitation factors, which are mediated with the ABA signaling pathway.

Moreover, SnRK2 could activate downstream genes such as *ABF* [37]. Overexpression of *ABF* in *Arabidopsis* resulted in ABA hypersensitivity and high drought tolerance [38]. Meanwhile, upregulated *SnRK2* could activate several cation or anion channels, such as S-type anion channel 3 (*SLAH3*), to force stomata to close [34]. In the present study, the upregulation of *ABFs* indicated that the high expression level of *ABFs* in *B. striata* leaves could enhance the plant's drought tolerance under drought stress.

4.2. Effect of Drought Stress on DEGs Involved in Photosynthesis

As we mentioned above, nonstomatal limitation factors were the main reason for photosynthesis reduction. In other words, there was metabolic damage in the photosynthetic process, such as downregulation of gene expression of some photosynthesis-related proteins. Our transcriptional analyses found that four DEGs that participated in photosynthesis were downregulated. Cytochrome b6 was reported to function in regulating electron transfer between photosystem II and photosystem I [39]. The stability of *petB* transcripts could control cytochrome b6 levels. The transcriptional level of Cytochrome b6 (*petB*, Cluster-6724.91253) was decreased in our study, suggesting that the level of cytochrome b6 is reduced under drought stress and leads to an inhibition of electron transfer between photosystem II and photosystem I, which would result in low photosynthesis in *B. striata*. Photosystem I reaction center subunit III (*psaF*, Cluster-6724.49822) is a plastocyanin-docking protein participating in regulating efficiency of electron transfer from plastocyanin to P700 [40]. The lack of *psaF* results in an inability of energy transfer from light-harvesting complex I-730 to the P700 reaction center [40]. Photosystem I reaction center subunit IV (*psaE*, Cluster-6724.49802) participates in docking of ferredoxin to PSI and interaction with ferredoxin-NADP oxidoreductase [41]. Absence of *psaE* leads to low O_2 production and serious damage in PSII under photoinhibition conditions [41]. In other words, low transcriptional levels of *psaE* are adverse for plant photosynthesis. The downregulations of *psaE* and *psaF* in the present study imply that drought stress inhibits energy transfer and PSI assembling via regulating the expressions of *psaE* and *psaF* and subsequently affecting the photosynthesis of *B. striata*. As Krieger-Liszskav (2020) pointed out, high O_2 production protects PSII against photoinhibition [41]. Our transcriptomic data also found several DEGs related to O_2 production in *B. striata* leaves under drought stress. For example, psbP-domain-containing proteins (Cluster-6724.68113, Cluster-6724.86842, and Cluster-6724.74411) and psbQ proteins (Cluster-6724.44868 and Cluster-6724.11910) were reported to play a functional role in optimization of photosynthetic oxygen evolution [42,43]. Interestingly, all of these DEGs were upregulated, which will lead to higher efficiency of O_2 production, suggesting that *B. striata* might enhance O_2 production to protect its photosystem under drought stress. In addition, ATP-dependent zinc metalloprotease FtsH 11 (Cluster-6724.55459, Cluster-6724.47025) was found to be upregulated in *B. striata* leaves under drought stress (Table 3). In *Arabidopsis*, FtsH6 was found to participate in degradation of light-harvesting complex II during high-light acclimation [44].

Upregulation of FtsH11, a homologous protein, might have the same function in regulating degradation of light-harvesting complex II, which would lead to low efficiency of light-energy absorption. These changes in gene expression may be a self-protection mechanism for plants under drought stress.

4.3. Drought-Induced Gene Expression of Stress-Response Protein

When a plant is exposed to drought stress, many stress-responsive genes are induced to protect it from drought-induced damage [10]. Plants generally overaccumulate ROS in their tissues after any stressful insult, both biotic and abiotic. An antioxidant battery is the first line of defense against oxidative damage in plant cells [10]. The antioxidants commonly utilized by plants include catalase (CAT), superoxide dismutase (SOD), peroxidase (POX), ascorbate peroxidase (APX), glutathione sulfo-transferase (GST), and others [9]. As displayed in Table 3, almost all DEGs related to antioxidant metabolism were significantly upregulated except for APX. Overproduction of O_2^- is the first step undertaken by a plant under drought stress. SOD catalyzes O_2^- into the significantly less toxic H_2O_2 [12]. As more and more H_2O_2 is produced in a cell, it becomes reduced into H_2O with the enzymatic antioxidant CAT through electron transport, photorespiratory oxidation, and oxidation of fatty acids [7]. Alternatively, H_2O_2 can also be converted into H_2O with APX via the AsA-GSH cycle [7]. Under drought conditions, however, the expression level of APX was decreased, whereas the expression levels of SOD and CAT were increased, implying that ROS produced in drought-stressed *B. striata* leaves is mainly scavenged by SOD and CAT and not via the APX-mediated AsA-GSH cycle. In addition, POX was reported to minimize drought-induced cellular damage due to its ability to lignify and crosslink structural proteins in cell walls [11]. These results indicate that *B. striata* leaves reduce drought-induced oxidative damage via activating expressions of SOD, CAT, and POX to scavenge ROS.

Moreover, GO enrichment analysis identified six dehydrin (DHN) genes, which were highly expressed under drought stress (Figures 5 and 7). DHNs were initially recognized as “dehydration-induced proteins” in response to desiccation [45]. An increasing body of evidence suggests that DHN proteins impart drought stress tolerance through activating various biological processes, such as photosynthesis, ROS scavenging, accumulation of compatible solutes, and others [46]. Overexpression of DHNs could significantly enhance drought tolerance in plants. For example, overexpressions of two dehydrins, *Y2SK2* and *SK3*, in *Arabidopsis thaliana* resulted in higher tolerance of salt, osmotic cold, and drought stress, with higher antioxidant activity and photosynthesis [47]. In addition, DHN1 was reported to maintain high chlorophyll content and water fresh/dry weight but low H_2O_2 concentration, resulting from enhanced ROS scavenging [48]. Similar to these findings, we found that DHNs were significantly engaged in *B. striata* leaves under drought stress, implying that a high expression level of DHNs could enhance drought tolerance through enhancing ROS scavenging, which was consistent with our results of high expression levels of SOD, CAT, and POX.

5. Conclusions

B. striata is a valuable Chinese herbal medicinal plant. During the planting process, drought is one of the most serious threats to its growth and development. In the present study, the response of *B. striata* under drought stress was investigated at the physiological and transcriptional levels. Photosynthetic results indicated that the decline of photosynthesis in *B. striata* leaves was mainly caused by nonstomatal limitation factors. Transcriptomic analysis showed that DEGs involved in photosynthesis processes, such as electron transfer (cytochrome b6) and light-energy harvesting and transfer (photosystem I reaction center subunit III and photosystem I reaction center subunit IV), might lead to reduction in *B. striata* photosynthesis, while DEGs related to O_2 production (*psbP*, *psbQ*) and light-energy absorption (ATP-dependent zinc metalloprotease *FTSH 11*) are activated to protect the plant from drought stress. Moreover, the DEGs involved in the ABA signaling pathway were the most upregulated. Upregulations of *PP2C*, *SnRK2*, and *SLAH2* might lead to stomatal

closure, which is one of the reasons for photosynthesis reduction. In response to drought stress, the *B. striata* leaves recruited SOD, CAT, and POX, which enhanced the ability of ROS scavenging. High expressions of ABF and DHNs might result in high drought tolerance in *B. striata*. According to these results, a better understanding of *B. striata* in response to drought stress was presented in our study.

Supplementary Materials: The following supporting information can be downloaded at: <https://www.mdpi.com/article/10.3390/horticulturae9030307/s1>, Table S1: The detailed information of KEGG and GO enrichment analyses, Table S2: The information of DEGs involved in plant hormone signal transduction.

Author Contributions: Conceptualization, Z.S. and M.W.; methodology, H.L. and L.Y.; software, Z.S. and H.L.; validation, X.H., K.C. and Z.S.; formal analysis, M.W.; investigation, H.L. and K.C.; resources, M.W. and H.L.; data curation, M.W. and Z.S.; writing—original draft preparation, H.L. and K.C.; writing—review and editing, K.C., X.H., Z.S. and M.W.; visualization, H.L. and X.H.; supervision, Z.S. and M.W.; project administration, H.L. and M.W.; funding acquisition, M.W. All authors have read and agreed to the published version of the manuscript.

Funding: This research was funded by the National Key Research and Development Program of China (Grant No. 2021YFD1601002), the Guizhou Provincial Department of Science and Technology (Grant No. QKHFQ2020-4008, QKHZC2022-ZD023), the Modern Industrial Technology System of Chinese Medicinal Materials in Guizhou Province (No. GZCYTX2021-0202), the Natural Science Foundation of China (Grant No. 31401362), and the Major Science and Technology Program of Xiamen, China (Grant No. 3502Z20211004).

Data Availability Statement: The raw sequence data reported in this paper have been deposited in the Genome Sequence Archive (Genomics, Proteomics & Bioinformatics 2021) in the National Genomics Data Center (Nucleic Acids Res 2022), China National Center for Bioinformation/Beijing Institute of Genomics, Chinese Academy of Sciences (GSA: CRA008921), which is publicly accessible at <https://ngdc.cncb.ac.cn/gsa>.

Conflicts of Interest: The authors declare no conflict of interest.

References

- Gupta, A.; Rico-Medina, A.; Caño-Delgado, A.I. The physiology of plant responses to drought. *Science* **2020**, *368*, 266–269. [[CrossRef](#)] [[PubMed](#)]
- Hussain, M.; Malik, M.A.; Farooq, M.; Ashraf, M.Y.; Cheema, M.A. Improving Drought Tolerance by Exogenous Application of Glycinebetaine and Salicylic Acid in Sunflower. *J. Agron. Crop. Sci.* **2008**, *194*, 193–199. [[CrossRef](#)]
- Cattivelli, L.; Rizza, F.; Badeck, F.-W.; Mazzucotelli, E.; Mastrangelo, A.M.; Francia, E.; Marè, C.; Tondelli, A.; Stanca, A.M. Drought tolerance improvement in crop plants: An integrated view from breeding to genomics. *Field Crop. Res.* **2008**, *105*, 1–14. [[CrossRef](#)]
- Mckay, J.K.; Richards, J.H.; Mitchell-Olds, T. Genetics of drought adaptation in *Arabidopsis thaliana*: I. Pleiotropy contributes to genetic correlations among ecological traits. *Mol. Ecol.* **2003**, *12*, 1137–1151. [[CrossRef](#)]
- Prasad, P.V.V.; Staggenborg, S.; Ristic, Z. Impacts of drought and/or heat stress on physiological, developmental, growth, and yield processes of crop plants. *Adv. Agric. Syst. Model. Ser.* **2008**, *1*, 301–355.
- Shao, H.-B.; Chu, L.-Y.; Jaleel, C.A.; Zhao, C.-X. Water-deficit stress-induced anatomical changes in higher plants. *Comptes Rendus Biol.* **2008**, *331*, 215–225. [[CrossRef](#)]
- Laxa, M.; Liebthal, M.; Telman, W.; Chibani, K.; Dietz, K.-J. The Role of the Plant Antioxidant System in Drought Tolerance. *Antioxidants* **2019**, *8*, 94. [[CrossRef](#)]
- Corpas, F.J.; González-Gordo, S.; Palma, J.M. Plant Peroxisomes: A Factory of Reactive Species. *Front. Plant Sci.* **2020**, *11*, 853. [[CrossRef](#)]
- Lukatkin, A.S.; Anjum, N.A. Control of cucumber (*Cucumis sativus* L.) tolerance to chilling stress—evaluating the role of ascorbic acid and glutathione. *Front. Environ. Sci.* **2014**, *2*, 62. [[CrossRef](#)]
- Mukarram, M.; Choudhary, S.; Kurjak, D.; Petek, A.; Khan, M.M.A. Drought: Sensing, signalling, effects and tolerance in higher plants. *Physiol. Plant.* **2021**, *172*, 1291–1300. [[CrossRef](#)]
- Quan, L.-J.; Zhang, B.; Shi, W.-W.; Li, H.-Y. Hydrogen Peroxide in Plants: A Versatile Molecule of the Reactive Oxygen Species Network. *J. Integr. Plant Biol.* **2008**, *50*, 2–18. [[CrossRef](#)]
- Zandalinas, S.I.; Balfagón, D.; Arbona, V.; Gómez-Cadenas, A. Modulation of Antioxidant Defense System Is Associated with Combined Drought and Heat Stress Tolerance in Citrus. *Front. Plant Sci.* **2017**, *8*, 953. [[CrossRef](#)]

13. Chen, Z.; Cheng, L.; He, Y.; Wei, X. Extraction, characterization, utilization as wound dressing and drug delivery of *Bletilla striata* polysaccharide: A review. *Int. J. Biol. Macromol.* **2018**, *120*, 2076–2085. [[CrossRef](#)] [[PubMed](#)]
14. Zhang, C.; Gao, F.; Gan, S.; He, Y.; Chen, Z.; Liu, X.; Fu, C.; Qu, Y.; Zhang, J. Chemical characterization and gastroprotective effect of an isolated polysaccharide fraction from *Bletilla striata* against ethanol-induced acute gastric ulcer. *Food Chem. Toxicol.* **2019**, *131*, 110539. [[CrossRef](#)] [[PubMed](#)]
15. Liu, H.; Li, L.; Li, C.; Huang, C.; ShangGuan, Y.; Chen, R.; Xiao, S.; Wen, W.; Xu, D. Identification and bioinformatic analysis of Aox/IAA family based on transcriptome data of *Bletilla striata*. *Bioengineered* **2019**, *10*, 668–678. [[CrossRef](#)] [[PubMed](#)]
16. Niu, J.; Zhao, G.; Mi, Z.; Chen, L.; Liu, S.; Wang, S.; Wang, D.; Wang, Z. De novo sequencing of *Bletilla striata* (Orchidaceae) transcriptome and identification of genes involved in polysaccharide biosynthesis. *Genet. Mol. Biol.* **2020**, *43*, e20190417. [[CrossRef](#)] [[PubMed](#)]
17. Jiang, L.; Lin, M.; Wang, H.; Song, H.; Zhang, L.; Huang, Q.; Chen, R.; Song, C.; Li, G.; Cao, Y. Haplotype-resolved genome assembly of *Bletilla striata* (Thunb.) Reichb.f. to elucidate medicinal value. *Plant J.* **2022**, *111*, 1340–1353. [[CrossRef](#)]
18. Ding, L.; Shan, X.; Zhao, X.; Zha, H.; Chen, X.; Wang, J.; Cai, C.; Wang, X.; Li, G.; Hao, J.; et al. Spongy bilayer dressing composed of chitosan–Ag nanoparticles and chitosan–*Bletilla striata* polysaccharide for wound healing applications. *Carbohydr. Polym.* **2017**, *157*, 1538–1547. [[CrossRef](#)]
19. Wang, C.X.; Tian, M.; Li, Q.J.; Liu, F. Floral syndrome and breeding system of *Bletilla striata*. *Acta Hort. Sin.* **2012**, *39*, 1159–1166.
20. Zhang, M.; Shao, Q.; Xu, E.; Wang, Z.; Wang, Z.; Yin, L. *Bletilla striata*: A review of seedling propagation and cultivation modes. *Physiol. Mol. Biol. Plants* **2019**, *25*, 601–609. [[CrossRef](#)]
21. Liu, S.; Lu, C.; Jiang, G.; Zhou, R.; Chang, Y.; Wang, S.; Wang, D.; Niu, J.; Wang, Z. Comprehensive functional analysis of the PYL-PP2C-SnRK2s family in *Bletilla striata* reveals that BsPP2C22 and BsPP2C38 interact with BsPYLs and BsSnRK2s in response to multiple abiotic stresses. *Front. Plant Sci.* **2022**, *13*, 963069. [[CrossRef](#)] [[PubMed](#)]
22. Gao, Y.; Cai, C.; Yang, Q.; Quan, W.; Li, C.; Wu, Y. Response of *Bletilla striata* to Drought: Effects on Biochemical and Physiological Parameter Also with Electric Measurements. *Plants* **2022**, *11*, 2313. [[CrossRef](#)]
23. Larocque, G.R. Coupling a detailed photosynthetic model with foliage distribution and light attenuation functions to compute daily gross photosynthesis in sugar maple (*Acer saccharum* Marsh.) stands. *Ecol. Model.* **2002**, *148*, 213–232. [[CrossRef](#)]
24. Ramanjulu, S.; Sreenivasulu, N.; Sudhakar, C. Effect of Water Stress on Photosynthesis in Two Mulberry Genotypes with Different drought Tolerance. *Photosynthetica* **1998**, *35*, 279–283. [[CrossRef](#)]
25. Grabherr, M.G.; Haas, B.J.; Yassour, M.; Levin, J.Z.; Thompson, D.A.; Amit, I.; Adiconis, X.; Fan, L.; Raychowdhury, R.; Zeng, Q.D.; et al. Full-length transcriptome assembly from RNA-Seq data without a reference genome. *Nat. Biotechnol.* **2011**, *29*, 644–652. [[CrossRef](#)] [[PubMed](#)]
26. Li, B.; Dewey, C.N. RSEM: Accurate transcript quantification from RNA-Seq data with or without a reference genome. *BMC Bioinform.* **2011**, *12*, 323. [[CrossRef](#)] [[PubMed](#)]
27. Benjamini, Y.; Drai, D.; Elmer, G.; Kafkafi, N.; Golani, I. Controlling the false discovery rate in behavior genetics research. *Behav. Brain Res.* **2001**, *125*, 279–284. [[CrossRef](#)]
28. Weyers, J.D.B.; Paterson, N.W. Plant hormones and the control of physiological processes. *New Phytol.* **2001**, *152*, 375–407. [[CrossRef](#)]
29. Kazan, K. Diverse roles of jasmonates and ethylene in abiotic stress tolerance. *Trends Plant Sci.* **2015**, *20*, 219–229. [[CrossRef](#)]
30. Ullah, A.; Manghwar, H.; Shaban, M.; Khan, A.H.; Akbar, A.; Ali, U.; Ali, E.; Fahad, S. Phytohormones enhanced drought tolerance in plants: A coping strategy. *Environ. Sci. Pollut. Res.* **2018**, *25*, 33103–33118. [[CrossRef](#)]
31. Danquah, A.; de Zelicourt, A.; Colcombet, J.; Hirt, H. The role of ABA and MAPK signaling pathways in plant abiotic stress responses. *Biotechnol. Adv.* **2014**, *32*, 40–52. [[CrossRef](#)] [[PubMed](#)]
32. Ullah, A.; Sun, H.; Yang, X.; Zhang, X. Drought coping strategies in cotton: Increased crop per drop. *Plant Biotechnol. J.* **2017**, *15*, 271–284. [[CrossRef](#)] [[PubMed](#)]
33. Yoshida, R.; Hobo, T.; Ichimura, K.; Mizoguchi, T.; Takahashi, F.; Aronso, J.; Ecker, J.; Shinozaki, K. ABA-Activated SnRK2 Protein Kinase is Required for Dehydration Stress Signaling in *Arabidopsis*. *Plant Cell Physiol.* **2002**, *43*, 1473–1483. [[CrossRef](#)]
34. Bharath, P.; Gahir, S.; Raghavendra, A.S. Abscisic Acid-Induced Stomatal Closure: An Important Component of Plant Defense Against Abiotic and Biotic Stress. *Front. Plant Sci.* **2021**, *12*, 615114. [[CrossRef](#)]
35. Mori, I.C.; Murata, Y.; Yang, Y.; Munemasa, S.; Wang, Y.-F.; Andreoli, S.; Tiriack, H.; Alonso, J.M.; Harper, J.F.; Ecker, J.R.; et al. CDPKs CPK6 and CPK3 Function in ABA Regulation of Guard Cell S-Type Anion- and Ca²⁺- Permeable Channels and Stomatal Closure. *PLoS Biol.* **2006**, *4*, 1749–1762. [[CrossRef](#)] [[PubMed](#)]
36. Flexas, J.; Medrano, H. Drought-inhibition of photosynthesis in C3 plants: Stomatal and non-stomatal limitations revisited. *Ann. Bot.* **2002**, *89*, 183–189. [[CrossRef](#)] [[PubMed](#)]
37. de Ollas, C.; Dodd, I.C. Physiological impacts of ABA–JA interactions under water-limitation. *Plant Mol. Biol.* **2016**, *91*, 641–650. [[CrossRef](#)] [[PubMed](#)]
38. Fujita, Y.; Fujita, M.; Satoh, R.; Maruyama, K.; Parvez, M.M.; Seki, M.; Hiratsu, K.; Ohme-Takagi, M.; Shinozaki, K.; Yamaguchi-Shinozaki, K. AREB1 Is a Transcription Activator of Novel ABRE-Dependent ABA Signaling That Enhances Drought Stress Tolerance in *Arabidopsis*. *Plant Cell* **2005**, *17*, 3470–3488. [[CrossRef](#)]

39. Stoppel, R.; Lezhneva, L.; Schwenkert, S.; Torabi, S.; Felder, S.; Meierhoff, K.; Westhoff, P.; Meurer, J. Recruitment of a Ribosomal Release Factor for Light- and Stress-Dependent Regulation of *petB* Transcript Stability in *Arabidopsis* Chloroplasts. *Plant Cell* **2011**, *23*, 2680–2695. [[CrossRef](#)]
40. Haldrup, A.; Simpson, D.J.; Scheller, H.V. Down-regulation of the PSI-F Subunit of Photosystem I (PSI) in *Arabidopsis thaliana*—The PSI-F subunit is essential for photoautotrophic growth and contributes the antenna function. *J. Biol. Chem.* **2000**, *275*, 31211–31218. [[CrossRef](#)]
41. Krieger-Liszakay, A.; Shimakawa, G.; Sétif, P. Role of the two PsaE isoforms on O₂ reduction at photosystem I in *Arabidopsis thaliana*. *Biochim. Biophys. Acta (BBA)—Bioenerg.* **2019**, *1861*, 148089. [[CrossRef](#)] [[PubMed](#)]
42. Bricker, T.M.; Roose, J.L.; Zhang, P.; Frankel, L.K. The PsbP family of proteins. *Photosynth. Res.* **2013**, *116*, 235–250. [[CrossRef](#)] [[PubMed](#)]
43. Kakiuchi, S.; Uno, C.; Ido, K.; Nishimura, T.; Noguchi, T.; Ifuku, K.; Sato, F. The PsbQ protein stabilizes the functional binding of the PsbP protein to photosystem II in higher plants. *Biochim. Biophys. Acta (BBA)—Bioenerg.* **2012**, *1817*, 1346–1351. [[CrossRef](#)] [[PubMed](#)]
44. Želisko, A.; García-Lorenzo, M.; Jackowski, G.; Jansson, S.; Funk, C. AtFtsH6 is involved in the degradation of the light-harvesting complex II during high-light acclimation and senescence. *Proc. Natl. Acad. Sci. USA* **2005**, *102*, 13699–13704. [[CrossRef](#)]
45. Close, T.J.; Kortt, A.A.; Chandler, P.M. A cDNA-based comparison of dehydration-induced proteins (dehydrins) in barley and corn. *Plant Mol. Biol.* **1989**, *13*, 95–108. [[CrossRef](#)]
46. Riyazuddin, R.; Nisha, N.; Singh, K.; Verma, R.; Gupta, R. Involvement of dehydrin proteins in mitigating the negative effects of drought stress in plants. *Plant Cell Rep.* **2021**, *41*, 519–533. [[CrossRef](#)]
47. Yang, Z.; Sheng, J.; Lv, K.; Ren, L.; Zhang, D. Y2SK2 and SK3 type dehydrins from *Agapanthus praecox* can improve plant stress tolerance and act as multifunctional protectants. *Plant Sci.* **2019**, *284*, 143–160. [[CrossRef](#)]
48. Verma, G.; Dhar, Y.V.; Srivastava, D.; Kidwai, M.; Chauhan, P.S.; Bag, S.K.; Asif, M.H.; Chakrabarty, D. Genome-wide analysis of rice dehydrin gene family: Its evolutionary conservedness and expression pattern in response to PEG induced dehydration stress. *PLoS ONE* **2017**, *12*, e0176399. [[CrossRef](#)]

Disclaimer/Publisher’s Note: The statements, opinions and data contained in all publications are solely those of the individual author(s) and contributor(s) and not of MDPI and/or the editor(s). MDPI and/or the editor(s) disclaim responsibility for any injury to people or property resulting from any ideas, methods, instructions or products referred to in the content.